NASA Technical Memorandum 87803

The Geoscience Laser Altimetry/Ranging System (GLARS)

Steven C. Cohen, John J. Degnan,
Jack L. Bufton, James B. Garvin,
James B. Abshire

SEPTEMBER 1986

(NASA-TM-87803) THE GEOSCIENCE LASER ALTIMETRY/RANGING SYSTEM (GLARS) (NASA) 19 p CSCL 20E

N87-14687

Unclas
G3/36 43757

NASA

NASA Technical Memorandum 87803

The Geoscience Laser Altimetry/Ranging System (GLARS)

Steven C. Cohen, John J. Degnan,
Jack L. Bufton, James B. Garvin,
James B. Abshire

National Aeronautics and
Space Administration

**Scientific and Technical
Information Branch**

1986

CONTENTS

INTRODUCTION

Satellite based applications of ranging measurements have become increasingly more sophisticated during the last decade to the point where ranging data to and from satellites provide some of the most accurate geodetic measurements from which geophysically interesting parameters can be deduced. For example, satellite laser ranging observations from a global network of ground observatories to such satellites as Lageos and Starlette are being used to observe nearly instantaneous tectonic plate motion and crustal deformations at seismically active tectonic plate boundaries (e.g., Christodoulidis et al., 1985; Tapley et al., 1985; Cohen, 1985). The laser tracking data also provide highly accurate polar motion and earth rotation information (Smith et al., 1985, Tapley et al., 1985). Perturbations in satellite orbits determined by laser ranging data have been studied to deduce solid earth and oceanic tides (Lambeck, 1980), mantle viscosity (Peltier, 1983, Rubincam, 1984), and other geophysically interesting parameters (Cohen and Smith, 1985 and references therein). Similarly, satellite based radar altimetric data have been used to map the ocean surface, to study the variability in sea heights, to relate geoid heights to the dynamics of plate motion and mantle convection, and to study ice sheet topography (cf. Seasat Special Issue, 1983). Both data sets, along with Doppler data and other ranging data, are used in the derivation of global gravity field models such as the GEM (Lerch et al., 1982) and the GRIM (Reigber et al., 1985) models. Recently, topographic mapping of land surfaces from space has attracted much interest (Burke and Dixon, 1986).

Despite the success of satellite laser ranging as one of the most important data sources for high precision geodetic studies, the measurement program is limited by the number of (expensive to build and operate) ground tracking observatories. Several years ago a number of investigators (Fitzmaurice et al., 1975; Vonbun et al.; 1977, Kumar and Mueller, 1978; Cohen and Cook, 1979; Kahn et al., 1980) proposed to overcome this limitation by inverting the traditional satellite laser ranging system with the ranging hardware being placed onboard a satellite and the passive targets placed on the ground. Simulation studies showed the particular utility of such a system for studying regional and local scale crustal movements over baselines extending up to 1000 km. Engineering studies indicated the system was technically achievable (Degnan, 1984). Nevertheless, during the last decade more effort has been devoted to improving ground-based satellite laser ranging (SLR), very-long-baseline-interferometry (VLBI), and more recently, the Global Positioning System (GPS) than to developing spaceborne laser ranging. A lunar laser altimeter was successfully flown on Apollo 17, however, neither the vertical accuracy nor the horizontal resolution were of the quality required for contemporary geodynamic and geophysical studies on the Earth. Three recent developments make the present time one of renewed interest in a GLARS. First, SLR and VLBI systems have become operational, and the GPS will become fully so within the next few years. The high precision data being acquired by these systems suggest that even greater dividends can accrue from studies of crustal movements both over shorter baselines than readily surveyed by these systems and at more frequent rates. Second, the development of plans by NASA to launch and maintain both the Space Station and the Earth Observing System (Eos) in the 1990's provide an advantageous scenario for implementing a GLARS at modest cost and with minimal risk. Third, the continued development of system components and capabilities (e.g., diode pumped lasers, efficient frequency doubling and tripling crystals, and streak tube detectors) now make the development of the combined laser ranging and altimeter system particularly viable.

Earth Observing System

Because much of the recent impetus for the development of GLARS now comes from preparation for the Eos mission, it is appropriate to briefly review some of the conceptual characteristics of this system. It should be understood that Eos plans are still evolving, that the authors are not involved in the overall Eos design, and that their views do not express official NASA policy about Eos. Nonetheless, we have been involved in some of the instrument panel studies for Eos, particularly those involved with laser remote sensing. Furthermore, in the present paper, it is necessary to consider only some of the most essential features of Eos and its planned orbit. Clearly, Eos is motivated by the realization that a detailed study of the earth requires data from a variety of sensors (NASA, 1984). The sensors must be available for global and continuous data collection when appropriate. Furthermore, data interpretation will often require merging of information from several sensors and from both space and ground observatories (Earth System Sciences Committee, 1986). Accordingly, in the Eos concept, up to as many as four large, multisensor platforms will be placed into earth orbit. Among the sensors likely to be included are multiband medium and high resolution spectrometers, microwave radiometers, synthetic aperture radars, scatterometers, lidars, atmospheric composition monitors, altimeters, etc. Different sensors may be placed on different platforms depending on the sensor characteristics, synergistic science, and weight and power budgets. Most of the orbits being considered for Eos are sun synchronous, nearly polar orbits of the type generally considered for systematic mapping of the earth's surface (however lower inclination orbits are also being considered). Altitudes being considered range from a few hundred kilometers to 800–900 kilometers. Although the platform design has not been determined, weights of 10 to 15 thousand kilograms are being considered. Correspondingly the platforms are likely to have large spatial dimensions. The experiments will be serviceable on about a two year basis.

This will allow for equipment replacement and upgrading. GLARS fits very well into the Eos concept. For geodynamic purposes observations of ground movements should be made at least quarterly near seismic zones during times of low seismic and geodetic activity and nearly continuously when substantial activity is noted. Nevertheless, the overall duty cycle for geodynamic ranging observations is relatively small. Altimetric mapping of the topography and roughness of ice sheets, land surfaces, and the ocean require a fuller duty cycle for global surveys but only limited resurveying. The planned GLARS system allows for either simultaneous or non-simultaneous ranging and altimetric operation. The system is relatively lightweight, compact, and modest in power requirements so it can be accommodated into a variety of experimental complements on Eos. The system can be operated from any altitude planned for Eos, although the higher orbits are preferred to minimize orbital perturbations.

SCIENTIFIC REQUIREMENTS FOR GLARS

All applications of GLARS make use of the measured round trip travel time for a laser pulse to traverse the distance between the transmitter/receiver and a target. With suitable processing of the data the travel time data can be converted into a range. For ranging to cube corner reflectors, the measured distance is the slant range from the satellite position at the time of pulse transmission, to the target, and back to the satellite at its position when the pulse is received. Figure 1 shows this mode of operation. For altimetry, the pulse is transmitted at the nadir angle and the measurement is, in essence, a determination of the height of the satellite above the target. The GLARS system discussed below can operate simultaneously in the ranging and altimetric modes and the two measurements involve a common use of many of the system components. Nevertheless, it is convenient to discuss the scientific requirements for the laser ranging and altimetric functions separately, recognizing all the while that they are a similar data type.

Laser Ranging Requirements

The primary driver for laser ranging applications is the desire for highly accurate relative position measurements in three dimensions for a moderately dense grid of targets to study crustal movements. For example, the monitoring of regional scale crustal movement requires that strain rates on

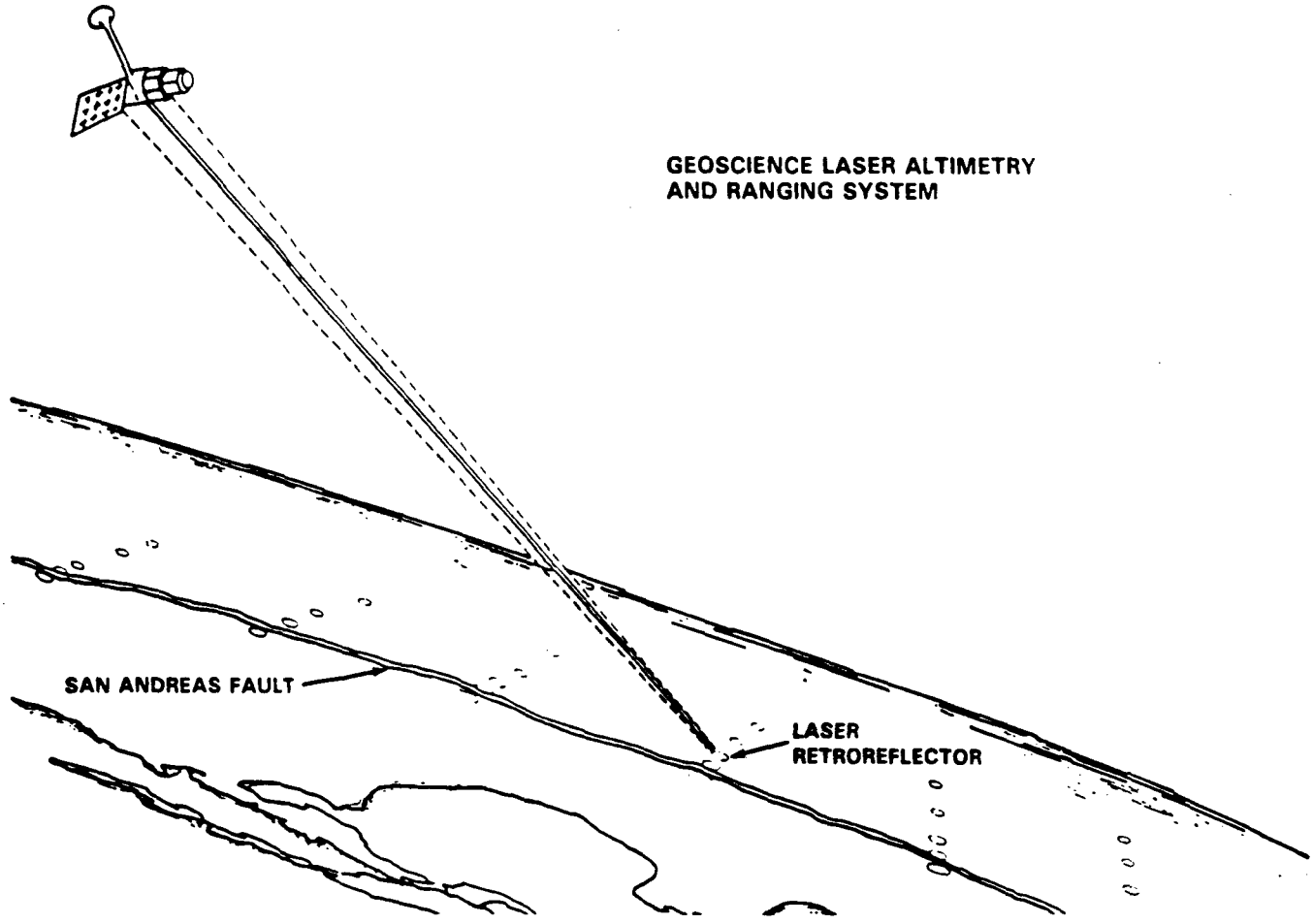

Figure 1. Conceptual representation of GLARS performing ranging measurements to cube corner retroreflectors.

the order of a few parts in 10^7 per year be determined within the vicinity of an active fault; smaller rates must be measured farther away (Savage, 1983). A strain rate precision of a few parts in 10^7 per year is equivalent to a change in intersite length of a few millimeters per year for a single line 50 kilometers long. Generally, an entire network of lines must be surveyed to determine the full strain tensor. To ensure high data quality and to search for temporal variations in crustal strain, we anticipate that GLARS measurements would be made at least quarterly in seismic zones such as the San Andreas Fault System in California. At times, however, crustal deformation may be much more rapid than suggested by interseismic strain accumulation. Movements of several centimeters or more can occur in hours to a few days prior to or following a major earthquake or in a creep event. More generally, relative displacements varying from millimeters to meters occur across baselines of less than a kilometer to hundreds of kilometers over temporal periods ranging from several hours to several years during various phases of the earthquake strain accumulation and release cycle (Cohen and Kramer, 1984). Thus, one of the requirements placed on GLARS observations is that the relative positions of sites be obtainable with subcentimeter precision; the baseline lengths may be up to several hundred kilometers long and the time span for resurveying as short as a few days. On a longer time scale (years to decades and longer) the positions and velocities of ground targets should be tied to a global geodetic coordinate system with the three dimensional target coordinates obtained to an accuracy of a few centimeters or better in a global solution. Several other applications of the ranging type observations require similar accuracies. For example, monitoring of land subsidence and uplift due to both natural and artificial effects requires relative height determinations of several centimeters or better. Similarly the measurement of target velocities and intersite strains on ice sheets are important for understanding their growth, decay, and dynamics (Thomas et al., 1985). These, in turn, are important for understanding the global hydrologic cycle and climate changes. The ranging data are also important for defining a highly accurate satellite ephemeris. The ephemeris is needed for the reduction of high precision laser altimeter measurements using GLARS, radar altimetry measurements, and other position sensitive instrument measurements

Laser Altimeter Requirements

Whereas the ranging measurements are designed to determine retroreflector positions and intersite distances, the altimetric measurements determine the spacecraft height above the earth's surface. If the spacecraft altitude is also known, then the height of the feature being observed is determined. One of the primary applications of the altimeter is mapping solid earth topography, a basic data set for geological and geodynamic studies. The required vertical precision for the overland topographic mapping is 10 to 50 cm (Dixon and Burke, 1986) with the horizontal resolution about 70–100 meters. Among the important geological applications are the characterization of desert topography and measurement of sand sheet mass transport, the determination of thicknesses of lava flows and the measurement of quaternary geologic features including debris flows, landslides, and impact craters. In addition, the GLARS topographic data would be used in conjunction with other topographic and gravity data in determinations of the earth's global figure and lithospheric flexure. The mapping of the topography of ice sheets provides information for deducing the ice thicknesses and for studying how the ice sheets are created and destroyed. Over oceans, short wavelength, high resolution, decimeter level topography is important for modeling oceanic dynamic processes. Hydrological applications (which involve determining energy balance by calculating the reflection of radiation off the earth's surface) require that slopes be mapped from height data with an accuracy of a few tens of centimeters over distances of seveal hundred kilometers. In the case of altimetric mapping over efficient reflectors such as ice sheets, the GLARS system will also have the capability to measure the vertical distribution within a single target spot. Such roughness studies would aid in the description of ice sheets and geological features, the study of underlying physical processes responsible for height variations, and the calibration of radar-derived roughnesses in the centimeter to decimeter wavelength range.

Both ranging and altimetric requirements can be satisfied by an ultrashort pulse, modest power laser ranging system whose specifications are given in Table 1. The system must have precision pointing capability and a lifetime of about 10^9 pulses. Multicolor operation is desired in the ranging application to minimize errors in computed ranges due to refractive index uncertainties.

SYSTEM DESCRIPTION

A block diagram of the planned GLARS instrument is illustrated in Figure 2. The system consists of three major subsystems: (1) a dual mode laser ranging/altimetry subsystem; (2) a high speed, high accuracy optical tracking subsystem; and (3) a navigation and attitude determination subsystem. Over the past decade, functional engineering prototypes of the laser ranging and optical pointing systems have been designed, fabricated, integrated and tested successfully (Degnan, 1984). Autonomous short pulse laser altimeters have also flown in a variety of high altitude research aircraft. Some additional development will be required in certain components, principally the laser transmitter and streak-camera receiver, to achieve full space-qualified status for the system prior to Eos launch.

The laser transmitter consists of a subnanosecond pulse Nd:YAG laser oscillator, double and single pass Nd:YAG amplifiers, a KD*P frequency doubling crystal, and a KD*P

Table I. GLARS Technical Specifications

Laser: frequency doubled and tripled, mode locked Nd:YAG

Pulsewidth: 100 picoseconds (FWHM)

Energy: 120 millijoules (1064 nm)
60 millijoules (532 nm)
20 millijoules (354 nm)

Beam divergence: 0.1 millirad

Ground spot diameter: 80 meters (800 km range)

Maximum pulse repetition rate: 40 pps

Ground spot spacing (altimetry mode): 650 meters at 10 pps
160 meters at 40 pps

Receiver telescope diameter: Ranging function: 18 cm
Altimetry function: 50 cm

Receiver electronic systems:
1. Si avalanche photodiode detector constant fraction discriminator waveform digitizer
2. photomultiplier (450 picosecond) constant fraction discriminator event timer (20 picosecond) streak tube (2 picosecond)

Ranging mirror tracking precision: 0.01 milliradians

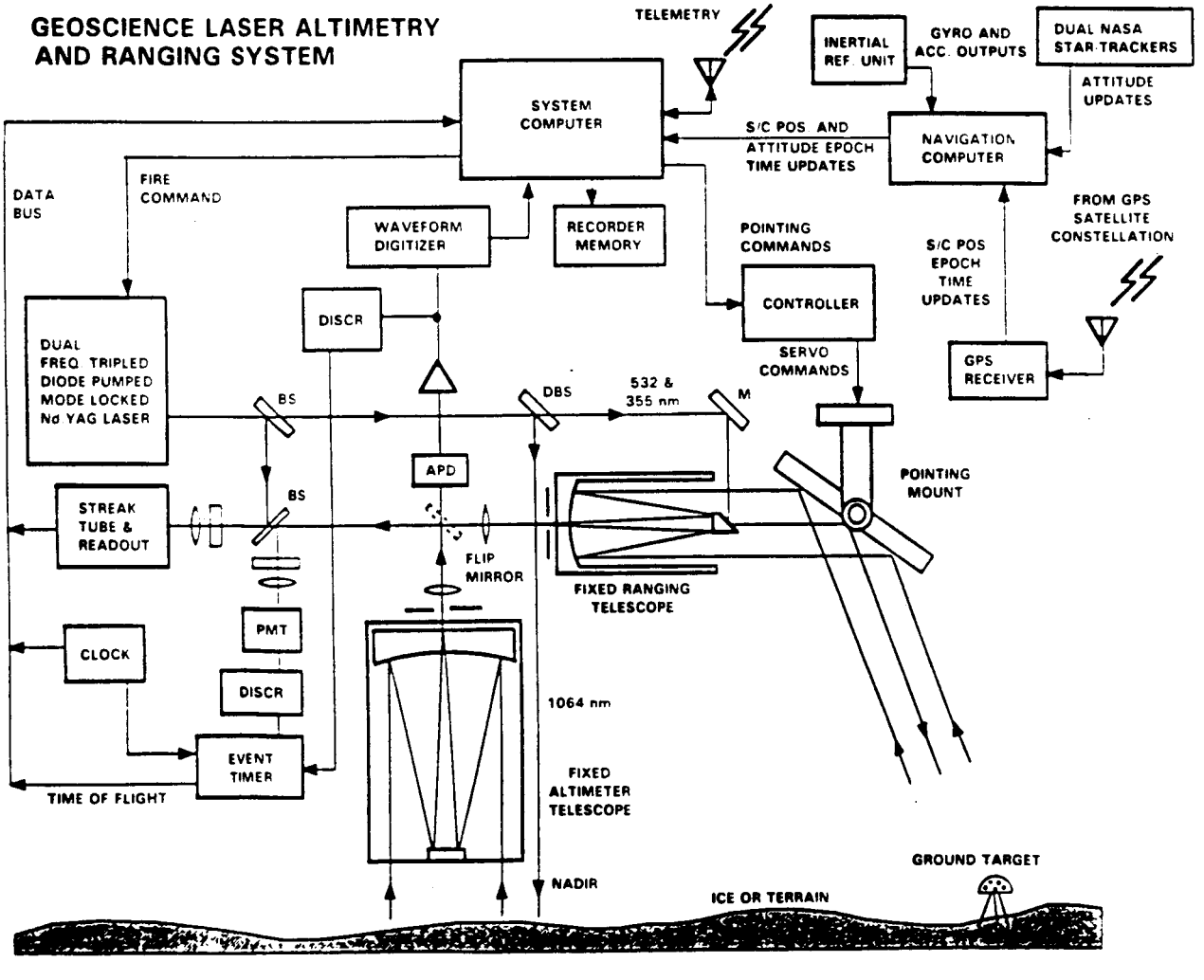

Figure 2. Block diagram of GLARS system.

frequency tripling crystal. The Nd:YAG laser operates at a fundamental near infrared wavelength of 1064 nm. The passive frequency doubling and tripling crystals produce subnanosecond pulses at the 532 nm green and the 355 nm near ultraviolet wavelengths, respectively. The visible and ultraviolet outputs are dedicated to the ranging application while the remaining infrared radiation is allocated to the altimetry function. The use of aluminum-gallium-arsenide laser diode arrays to pump the Nd:YAG laser medium offers potentially longer operational lifetimes, greater prime power efficiency, and smaller, lighter weight instrumentation when compared to conventional flashlamp pumped lasers. Referring to Figure 2, the ultrashort infrared laser pulse is stripped from the green and ultraviolet laser radiation by a dichroic mirror and directed toward nadir and the underlying terrain for altimetry measurements. The green and ultraviolet pulses are directed into the retroranging channel. A small fraction of the outgoing green laser pulse is deflected by beam splitters into the range receiver to start the time of flight measurement for both the ranging and altimetry functions. The remaining green and ultraviolet radiation is directed to a high speed, arcsecond-accuracy optical pointing mount. The two pulses propagate through the atmosphere to the retroflector and back. The returned radiation is reflected from the pointing mirror into a fixed 18 cm diameter Cassegrain collecting telescope which focuses the light through a spatial filter into the range receiver. A beam splitter directs a portion of the green return into a photomultiplier based receiver, while the remainder of the dual-wavelength signal is input to a picosecond resolution streak tube receiver. The photomultiplier receiver, described in more detail elsewhere (Degnan, 1985), measures the signal amplitudes and times-of-flight. The principal elements of the coarse receiver are a narrowband spectral filter, a high speed microchannel plate photomultiplier with a 450 picosecond impulse response, a low time walk constant fraction discriminator, and a 20 picosecond resolution event timer (Leskovar and Turko, 1978). The streak tube receiver acts as a picosecond resolution vernier on the coarse measurement of the green pulse time of flight. Furthermore, by measuring the temporal delay introduced between the green and ultraviolet stop pulses by atmospheric refraction with a few picoseconds resolution, the streak tube receiver can also determine the integrated refractive index seen by the pulses during their flight. This permits conversion of pulse time-of-flight to distance with an absolute accuracy of better than one centimeter (Abshire and Gardner, 1985). Since the streak tube records the entire returning waveform, it can also provide exceptionally high resolution measurement of visible wavelength altimetry returns from high reflectivity, low dispersion surfaces. This can be accomplished by steering the green output pulses to nadir via the optical pointing system and injecting the visible output of the larger altimeter telescope into the streak tube receiver by means of a computer-actuated flip mirror. The use of the larger telescope increases the signal-to-noise by roughly an order of magnitude.

In the altimetry channel, a fixed nadir-viewing 0.5 meter telescope collects the returning infrared altimetry signal and focuses it onto a high speed silicon avalanche photodiode detector (Si APD). The signal is amplified and split between a constant fraction discriminator and an electronic waveform digitizer. The discriminator generates a timing pulse whose time of arrival is recorded by the event timer along with the green retroranging pulses. This, combined with the time of departure of the outgoing green ranging pulse (which is simultaneous with the outgoing infrared pulse), provides the altimeter time of flight. The digitizer generates a one nanosecond resolution record of the returning infrared waveform and transmits it to the system computer for storage. This data provides information on surface slope and granularity and can be taken simultaneously with retroranging data. If simultaneous retroranging is not required, much higher resolution data can be achieved using streak tube records of the visible returns from highly reflective targets as mentioned previously.

The navigation and attitude determination subsystem consists of a navagation computer, inertial reference unit (IRU), a Global Positioning System (GPS) receiver, and twin standard NASA startrackers. Updated estimates of the spacecraft position at the meter level or better are provided periodically by the onboard GPS receiver with the spacecraft position between updates being obtained by integration of the dynamic equations of motion. Spacecraft attitude is maintained by a gyro triad in the IRU. The attitude determination software reads the output of the IRU sensors and integrates the equations of motion to yield current estimates of attitude. Long term drifts in the gyros are removed by periodic updates from the startrackers with precisions of a few tens of microradians.

Since the laser beam divergences planned for GLARS are about a tenth of a milliradian, the ground spots are about 70–100 meters wide on the ground. In the ranging mode, the absolute angular accuracy provided by the startrackers and GPS navigation system should permit open loop pointing to the ground retroreflectors. Nevertheless, the GLARS concept provides for an acquisition sequence if the system fails to detect range returns in the open loop mode. An optical pointing system is used to direct the outgoing ranging pulses to ground targets. The target locations are stored in the computer memory. Knowledge of the spacecraft and target positions and spacecraft attitude permits calculation of azimuth and elevation pointing angles in the instrument coordinate system. When a target is within the operating seventy degree angular range about nadir, the computer enables the firing of the transmitter at the desired repetition rate. The maximum fire rate is driven by the altimetry application where rates of 40 pps are required to provide nearly contiguous altimetry data for a nominal spacecraft altitude of 800

km. In the ranging application, rates of 10 pps are adequate for most purposes. In this mode, however, the pointing subsystem must be capable of slewing rapidly between ground targets and settling into arcsecond level tracking with a few seconds or less. The computational burden on the system computer is greatly reduced through the use of an intermediate microprocessor-based all digital controller to drive the optical tracking mount. The GLARS system computer provides angular position, velocity, and acceleration command updates approximately once a second to the controller. The controller, in turn, provides detailed commands to the drive motors at rates up to 512 times per second. An existing prototype of this system has a 200 degree/second maximum slew rate, a 500 degree/second^2 maximum angular acceleration and arcsecond tracking accuracy (Zagwodzki and White, 1986).

SIGNAL-TO-NOISE CONSIDERATIONS

More than a decade of experience in ground-based laser ranging to various satellites provides experimental proof that the required signal strength can be obtained at all altitudes considered for Eos. Link analyses for retroranging using GLARS indicate that 10–100 photoelectrons will be generated for every 10 millijoules of transmitted energy. The GLARS beam divergence of 0.1 milliradians assures that the targets can be readily acquired with sufficient energy being returned to the detection system. Mode locked operation is important in order to assure that the sharply defined waveform needed to obtain a ranging precision to one cm or better is achieved.

The pulse repetition rate is important to the GLARS ranging measurement in that it determines the number of observations that can be made on the targets. Typically, data can be acquired for about eight to ten minutes per revolution when a target grid is several hundred kilometers wide and observations are made to a slant angle of 20 degrees. Generally the satellite should be observed from at least three different angles per revolution. As an example, if the target grid consists of 80 retroreflectors the ranger should dwell on each target for approximately 2 seconds before slewing to the next target and make 3 passes through the entire grid during each data collection revolution. A total of 60 (240) observations will be made on a target per revolution when the pulse rate is 10 (40) pps. Typical Eos orbits result in four (sometimes three) potential data collection revolutions per day over each grid.

The laser altimeter concept described herein is based on a high signal-to-noise environment in which each laser pulse provides a unique range measurement (Bufton et al., 1982). It is important to preserve the independent data from each pulse in order to obtain horizontal topographic resolution of the order of 100 m while using laser pulse rates of 40 pps or less. Thus the altimetry performance analysis must verify that an adequate signal-to-noise ratio, S/N, can be expected for GLARS operation. For the altimeter the received signal energy E_R can be calculated from

$$E_R = E_T A_R T_O T_C^2 T_A^2 (r/w)/Z^2 \qquad (1)$$

where E_T is the transmitted laser energy, A_R the receiver area, Z the range to the surface, T_O the system optical transmission, T_C the cirrus cloud transmission, T_A the atmospheric aerosol transmission, and r/w the target backscatter. The number of photoelectrons produced by the received energy is obtained by multiplying this expression by the ratio of the detector quantum efficiency to the energy per photon (q/hv). Carrying out the calculations indicated in Eq. (1) requires specification of several empirical factors. First we consider the target backscatter, r/w. An ice-sheet is well modeled by a Lambertian reflectance and has values r/w of about 0.6 at 1064 nm (O'Brien, 1975). Soil and vegetation are lower in reflectance with r/w estimated in the range of 0.1/pi to 0.4/pi (Wolfe and Zizzis, 1978). The ocean surface exhibits a specular rather than diffuse reflectance. The range of variability of ocean backscatter is estimated from recent measurements to be equivalent to a reflectivity of 0.1/pi to 0.3/pi (Wolfe and Zizzis, 1978).

Cloud coverage is an important aspect of any satellite-based observations to the earth. Clearly the presence of significant cloud cover will disrupt laser altimetry measurements to the ground although cloud top heights may be measured in this circumstance. However thin cirrus clouds permit continued operation. Cloud models indicate that mid-latitude and polar regions generally have 40% to 50% cirrus cloud cover while the equatorial region has 80% cover. Calculations of the two-way propagation through typical cirrus cloud cover give transmission factors of 0.56 to 0.75 (Kneizys et al., 1983). Atmospheric transmission of the altimeter signal is affected by molecular scattering and by scattering and absorption due to lower tropospheric aerosols. There is little variability in molecular scattering at 1064 nm due to the inverse fourth power of wavelength dependence in Rayleigh scattering. Aerosol extinction on the other hand is significant in the atmospheric surface layer and is quite variable. Values of two way atmospheric transmission for currently available models are 0.2 to 0.8.

Considering these effects, the GLARS parameters given in Table I, a detector quantum efficiency of 0.3, and system transmission of 0.2 yields signal strengths between 100 and 4000 photoelectrons. These signal levels are sufficient for a high probability of detection for each altimeter pulse in the absence of noise.

Sources of noise in the altimetry measurement include scattered solar irradiance and detector noise. A solar illuminated cloud produces a worst-case source of background noise. Over a 10 nsec integration time the associated photoelectron count is

$$N_S = (q/hv)E_D(r/w)R_O T_R F_D A_R 10^{-8} \text{ sec} \qquad (2)$$

where E_D is the solar spectral irradiance (watt/m²/Angstrom), R_O is the receiver field of view (ster), T_R the receiver optical transmission, and F_D the filter bandpass (Angstrom). Taking the receiver field of view to be about 0.3 milliradians (to ensure collection of laser backscatter from the entire footprint) and an optical filter bandpass of 10 Å, the noise is 15 photoelectrons.

Considering all the aforementioned factors the signal to noise ratio for detection of the backscattered laser pulse can be written

$$S/N = N_R^2/((N_D + N_R)F + (N_D/G)^2) \quad (3)$$

where N_R is the mean signal photoelectron count, N_D the mean background photoelectron count, $(N_D/G)^2$ the variance of integrated detector dark current and preamplifier thermal noise (about 30 (photoelectrons)²), G the Si APD gain, and F a Si APD excess noise factor. Typical values for avalanche gain and excess noise factor are 250 and 5.7 respectively. These numbers result in a S/N of 19 to 690.

A finite S/N can cause a timing uncertainty in the altimetry measurement. The rms range error, ΔR, resulting from timing jitter in a maximum likelihood timing receiver is given by

$$\Delta R = c\Delta T/(2*\mathrm{sqrt}(S/N)) \quad (4)$$

where ΔT is the laser pulse width. With ΔT = 100 picoseconds, ΔR is less than 1 cm at all expected values of values of the signal-to-noise ratio. Hence, for altimetry measurements, the timing jitter due to low S/N does not appear to be the major problem. Probability of error and probability of false alarm are likely more serious effects at low S/N.

Another source of altimeter range uncertainty results from pulse spreading. The interaction of a finite laser beamwidth, b, an angular offset, Q, from nadir, and a surface slope, S, can produce significant spread, ΔT_S, beyond the nominal laser pulse width, ΔT. This spread can be determined from

$$\Delta T_S = (2/c)\mathrm{TAN}(Q + S)Z\ b \quad (5)$$

where c is the speed of light. Note that surface slope can either add a pulse spread or reduce it depending on slope polarity with respect to the angular offset from nadir. In some cases Q and S may approach 20 milliradians. For such cases ΔT_S approaches 10 nanoseconds. The original laser pulse width of 100 picoseconds can be spread by a factor of 100. Dealing with this pulse spreading makes waveform digitization and subsequent analysis of height variability within the returned signal an important aspect of GLARS altimetry. We estimate that a minimum of 10 signal photoelectrons must be obtained in each digitization interval in order to obtain a 10% precision in measurement of signal waveform amplitude in that interval. With an estimated 100 to 4000 signal photoelectrons available, as few as 10 or as many as 400 channels of digitization may be possible; these channels will be used to analyze the distribution of heights within the target footprint.

COVARIANCE ANALYSIS FOR RANGING OBSERVATIONS

One of the primary features of GLARS is the ability to determine simultaneously and with high accuracy the positions of and distances between many cube corner targets. As previously mentioned, this capability is particularly valuable for studying the regional and local scale straining and deformation in the vicinity of major seismic zones. To quantify this capability, a covariance error analysis was performed in which a typical measurement scenario was simulated. We considered an array of 157 cube corner targets arranged with 50 kilometer separations throughout the state of California as shown in Figure 3. Ranging observations were made to these targets whenever the targets were within a 70 degree cone about the satellite nadir. Figure 4 shows the ground tracks for the satellite for eleven orbits during which data could be collected over a three day interval using this scenario. A very simple data-collection logic was employed for simulation purposes. Initial target acquisition was completed within 15 seconds. Subsequently, observations were made on a target for 0.5 seconds (5 shots at 10 pulses/second). Slewing then advanced the laser beam onto the next available target in 0.5 seconds. Once the entire raster of visible targets had been scanned, the grid was again surveyed. In this manner, anywhere from one to six series of observations are made on each target during a pass over the grid. While the observation scheme can be made more sophisticated, this simple logic ensures viewing of the targets from the satellite at several different observing angles, an important consideration to obtain good survey accuracy. The simulation assumes that the satellite is in a circular orbit at an altitude of 824 km; the orbital inclination is 100 degrees. The single shot laser precision is assumed to be one cm. The other parameters used in the simulation are shown in Table II. The covariance analysis seeks to quantify the expected errors in the positions and baseline distances as a function of the laser precision, uncertainties in the geopotential coefficients, errors in drag, and errors in solar radiation pressure. In simultaneously adjusting the cube corner positions and the satellite orbit, we treat each pass of the satellite over the target grid as an independent arc. Thus our orbital arcs are quite short, in all cases less than 10 minutes. Figure 5a shows the computed uncertainty (accuracy) in the baseline distances, relative heights, and transverse displacements in a local coordinate system centered on station 79. This result depends only on the assumed noise in the laser system, the orbit geometry, station configuration, and measurement scenario. No model errors are considered. On the other hand, Figure 5b shows the estimated errors in the three displacement variables due to model uncertainties (aliasing). Considered are uncertainties in the gravity field, solar radiation pressure coefficient, drag coefficient, and GM. Although the gravity field effect is by far the most significant contributor to the bias, the choice of short arcs has minimized this effect as well as the

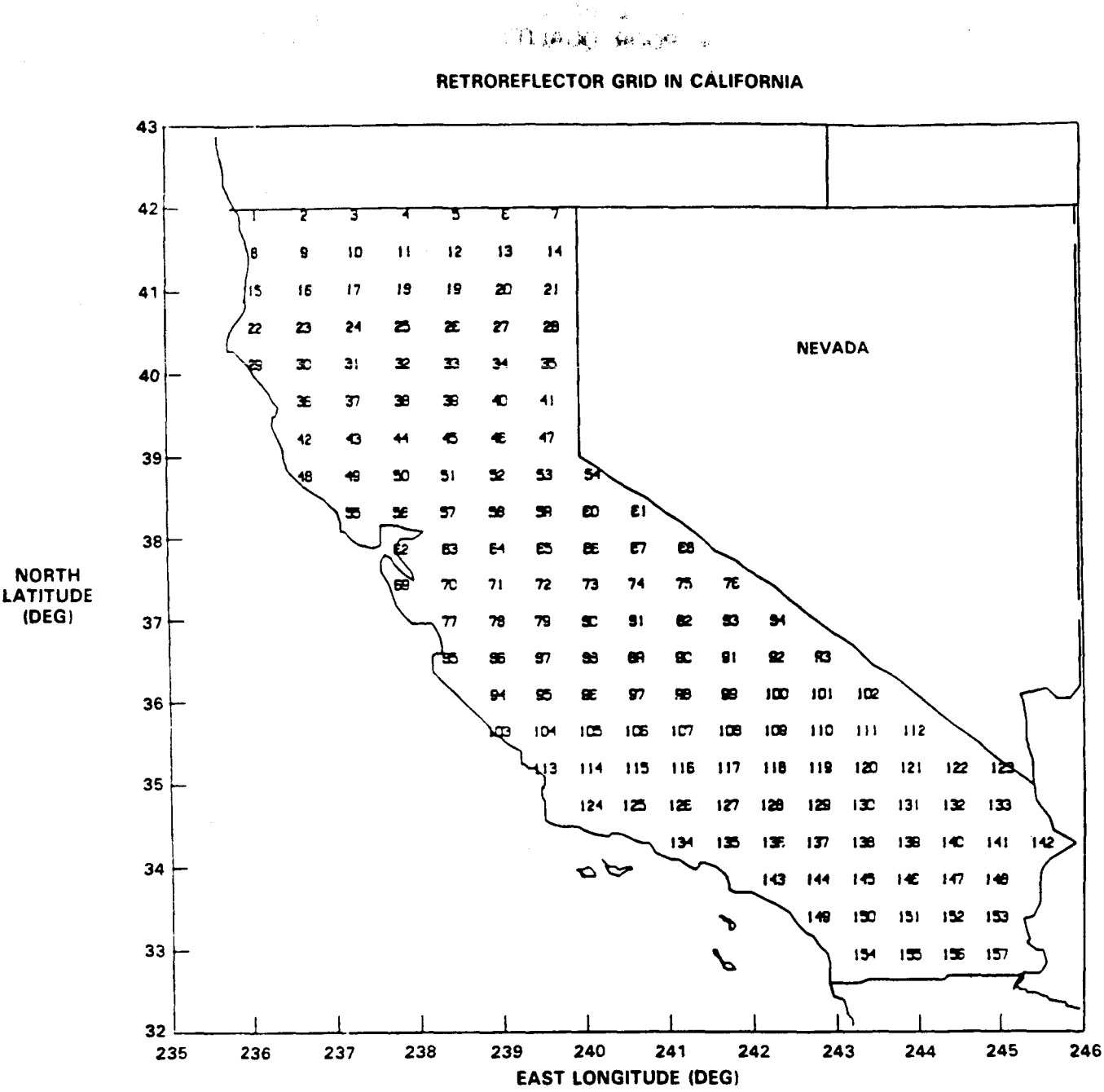

Figure 3. Retroflector locations for covariance analysis of ranging measurements.

Table II.
Parameters Used in Covariance Analysis

Laser ranging uncertainty: 1 cm	Gravity field: GEM 10B (to degree and order 22)
Retroreflector a priori position uncertainty: 1 meter	Gravity covariances: 0.25 × GEM10B covariances
Satellite a-priori position uncertainty: 1 meter	GM uncertainty: 1.333×10^7 m²/sec
Satellite a-priori velocity uncertainty: 1 mm/sec	Drag uncertainty: 20%
Orbital geometry: circular, 800 km altitude, 100° inclination	Solar radiation uncertainty: 33%
Data collection: 3 days (no loss due to cloud cover): 11 arcs	

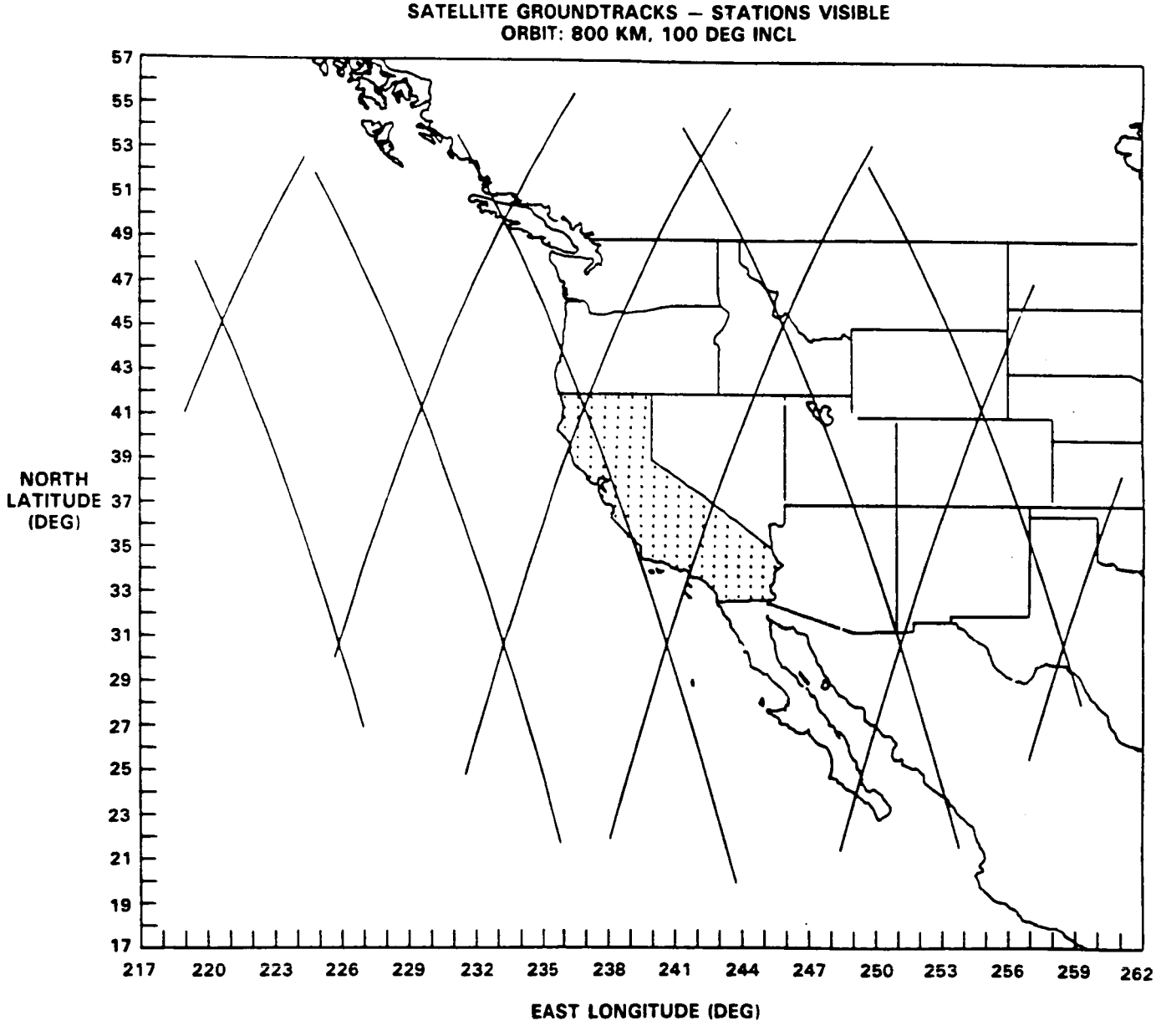

Figure 4. Ground tracks of orbits used in convariance analysis.

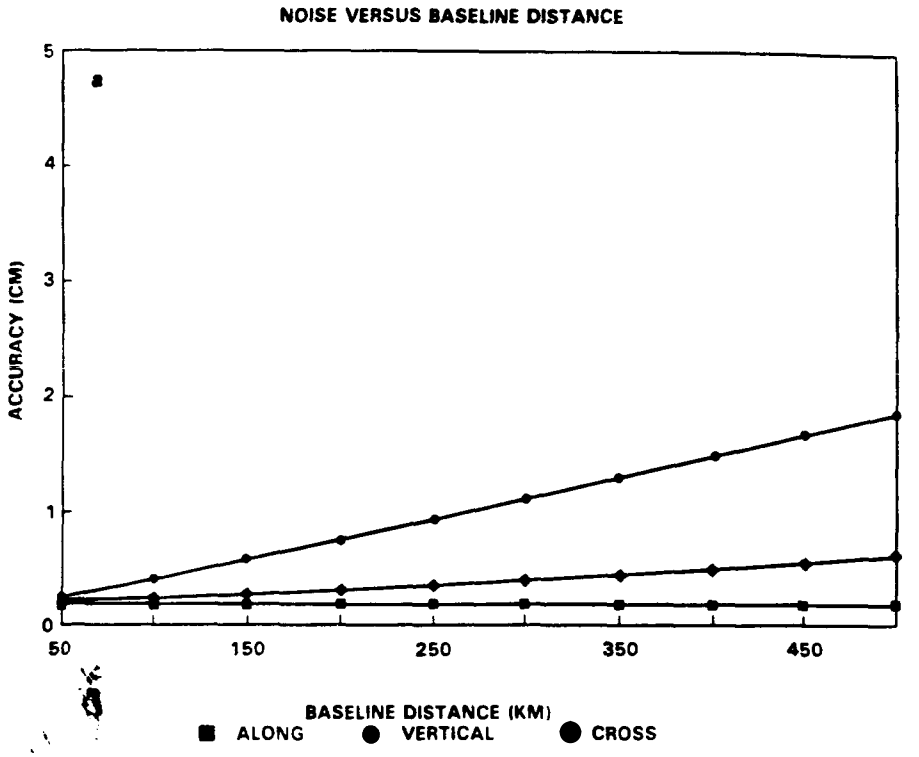

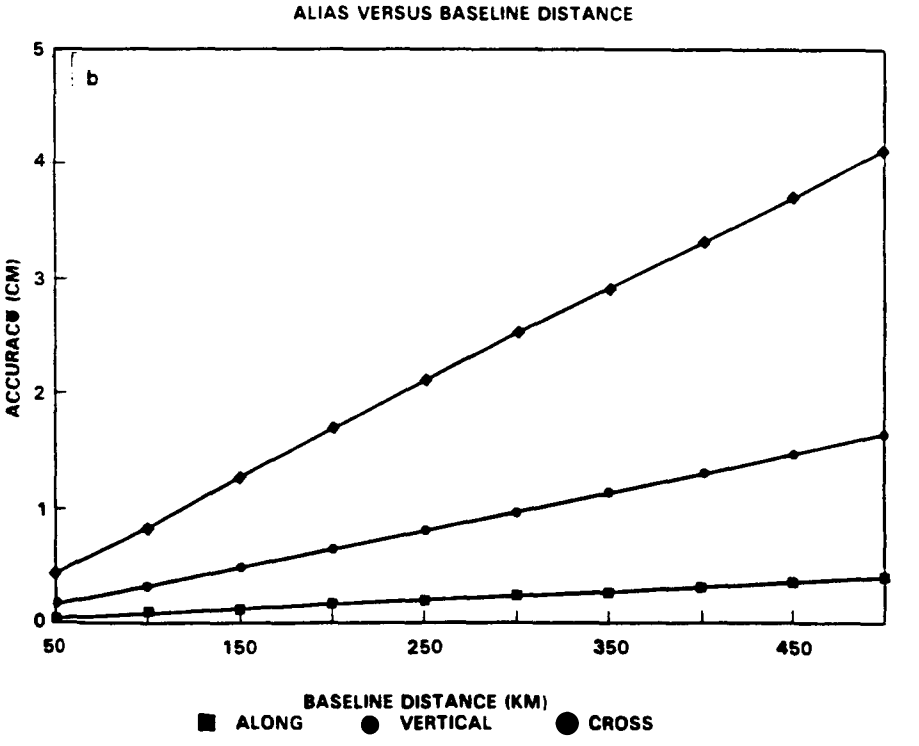

Figure 5. Covariance analysis of retroreflector position determinations from GLARS ranging data. The model parameters are given in Table II. The origin is site 79 and results are shown along a northerly path extending up to site 14.
a. Noise contribution to uncertainties in relative station positions.
b. Alias contribution to uncertainties in relative station positions.

aliasing due to uncertainties in drag and solar radiation pressure. The baseline accuracy is better than one centimeter even over distances longer than 500 km. By contrast, the aliasing in the baseline lengths resulting from arcs involving one or two complete orbits is about one to two centimeters at 500 km. The aliasing in the height and transverse displacement is significantly worse. The net uncertainty (in an accuracy sense) is the root of the sum of the noise only and alias contributions. For the short arc solution, the noise dominates the baseline uncertainty for distances out to 200–300 kilometers. At longer distances the alias effects become more significant. In any case, the computed baseline uncertainties are one cm or less for all distances out to 500 kilometers. The height uncertainties are somewhat larger at long distances, but still in the three to four centimeter range or less even at the longest distances we have studied. The aliasing in the cross track displacement is the largest of the components and ranges from less than one centimeter at 100 kilometers to over four centimeters at 500 kilometers. Since all of these results suggest a very highly precise and accurate system, we should emphasize that we do not claim that we have considered all possible effects at the several millimeter level of accuracy. It is reassuring, however, that those effects which have been found to be the most important for most geodetic missions do not preclude doing highly accurate geodesy at the centimeter level. It is also important that the baseline length is the most accurately determined component of the motion as the internal regional strain can often be derived solely from this parameter. In the environment of a strike slip fault, along much of the San Andreas fault in California, for example, horizontal motion dominates over vertical. Here the baseline data alone are sufficient to define the appropriate shear and normal stresses at the surface. However, in studying thrust faulting and orogenic processes vertical motion, is also important.

The results shown in Figure 5 are obtained along a northerly directed route between sites 79 and sites 14. On Figure 6 we compare these results with those computed for an eastwardly directed route between sites 79 and 84 (a total distance of 250 km). The predicted baseline uncertainty along the eastward directed route is slightly poorer than that for the northerly route. This is a reflection of the nearly polar orbital plane, which favors better resolution in the north-south direction. The results indicate, however, that even when the orbital plane is tilted only 10 degrees from an exact polar orbit, quite satisfactory recovery of baselines is obtained in both an east-west as well as north-south direction.

The solutions we have shown up to now give relative distances between a fixed origin within the network and other network points. There is also considerable interest in knowing the position of the grid points in a global coordinate system. For this purpose we use a coordinate system fixed on the earth's center of mass. In this system the noise only uncertainty in each of the coordinates is about seven to eight cm and is nearly uniform throughout the grid. Since much of the uncertainty is a common bias, there are much higher accuracies in the relative positions than in the coordinates relative to the center of mass. Similarly the uncertainties in the various coordinates due to gravity field uncertainties are in the range of 15–35 centimeters with high site correlations. The fact that a common bias dominates the solution in the earth-centered coordinate system suggests that once some of the targets are well-defined with respect to the center of the mass by other measurements, then the overall accuracy can be enhanced. This is, of course, the fiducial point concept. Fortunately, in many locales highly accurate fiducial points are available. In California, for example, fiducial points defined by satellite laser ranging and very long baseline interferometry sites of the Crustal Dynamics Project are already known with accuracies approaching one cm in appropriate coordinate systems. We can, therefore, repeat the covariance analysis assuming that certain sites are fiducial points. We have assumed, as a simple illustration, one cm a-priori uncertainties in the earth centered coordinates of sites 1, 113, and 123. Three results are obtained. First, the baseline distance determinations are relatively unaffected by the introduction of fiducial points, as they are accurately recovered by the internal adjustment alone. Conversely, the transverse (cross) displacements which had been weakly determined in the local solution are now more strongly determined. Finally, the most dramatic improvement is in the uncertainties of the site coordinates in the center of mass system (Figure 7). The a-priori constraints provide a reference frame for the network as a whole relative to the earth center of mass. The reference frame is much more accurately defined by the fiducial points than by the observations themselves. The observations, however, give the accurate position of the individual targets relative to the frame defined by the fiducial points. The net result is that all of the targets within the network become known at approximately the one centimeter level. We have intentionally chosen our fiducial points to avoid having three nearly collinear points and to form a triangle that spans much of the network. This, of course, makes the fiducial triangle a geodetically strong one. The availability of several well-constrained permanent observatories within California, western North America, Europe, and elsewhere makes achieving these constraint conditions quite likely.

From the standpoint of performing high precision altimetry it is essential to know accurately the satellite position during each of the observations. For GLARS, high precision positioning is enhanced by the system ranging observations, GPS positioning, and ground-based ranging to Eos. Currently, the orbital fit to observations on the high altitude (6000 km) Lageos satellite is better than 10 centimeters (D. E. Smith, private communication). Similarly, accuracies of

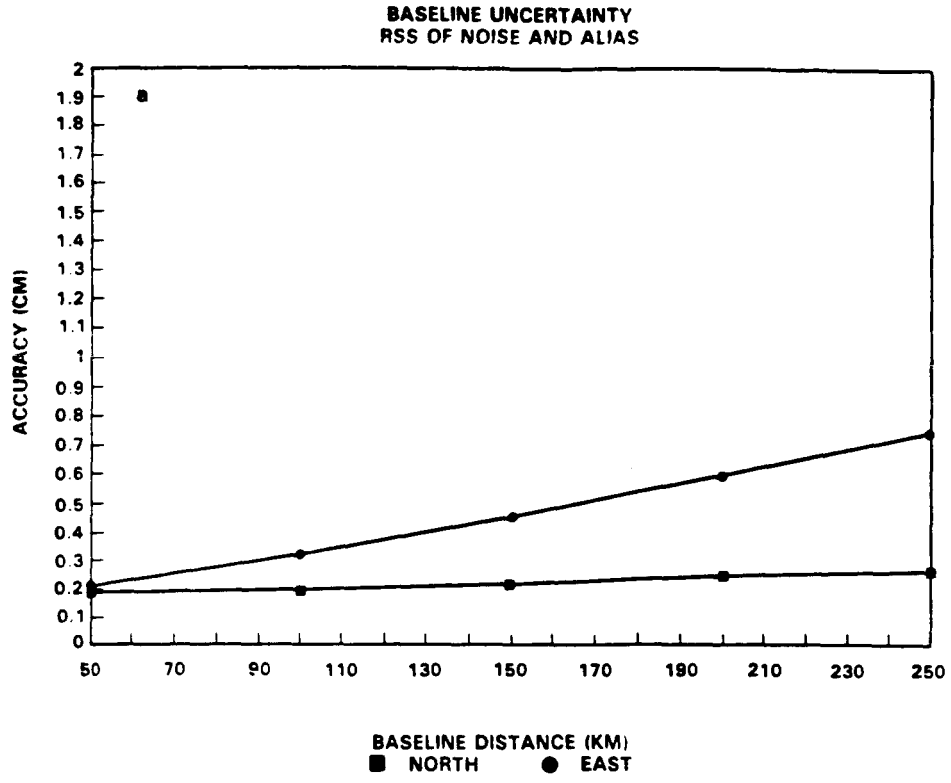

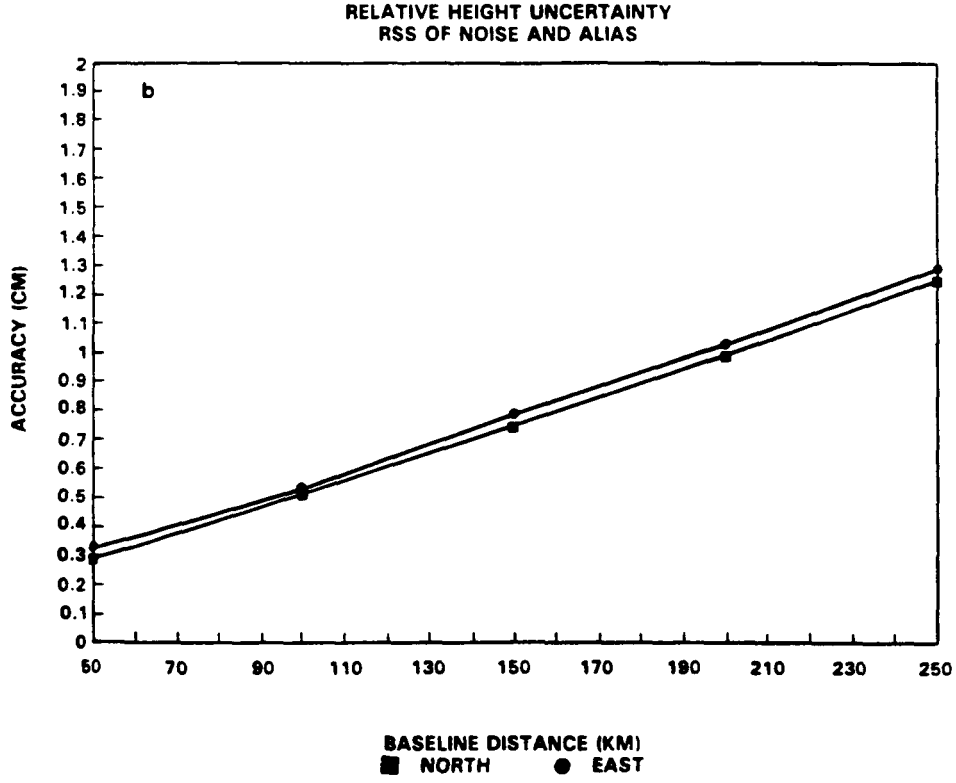

Figure 6a. Uncertainties (root sum of squares of noise and alias) in baselines along northerly path from site 79 to site 47 and along easterly path from site 79 to site 84.
b. Relative heights for same paths as in Figure 6a.

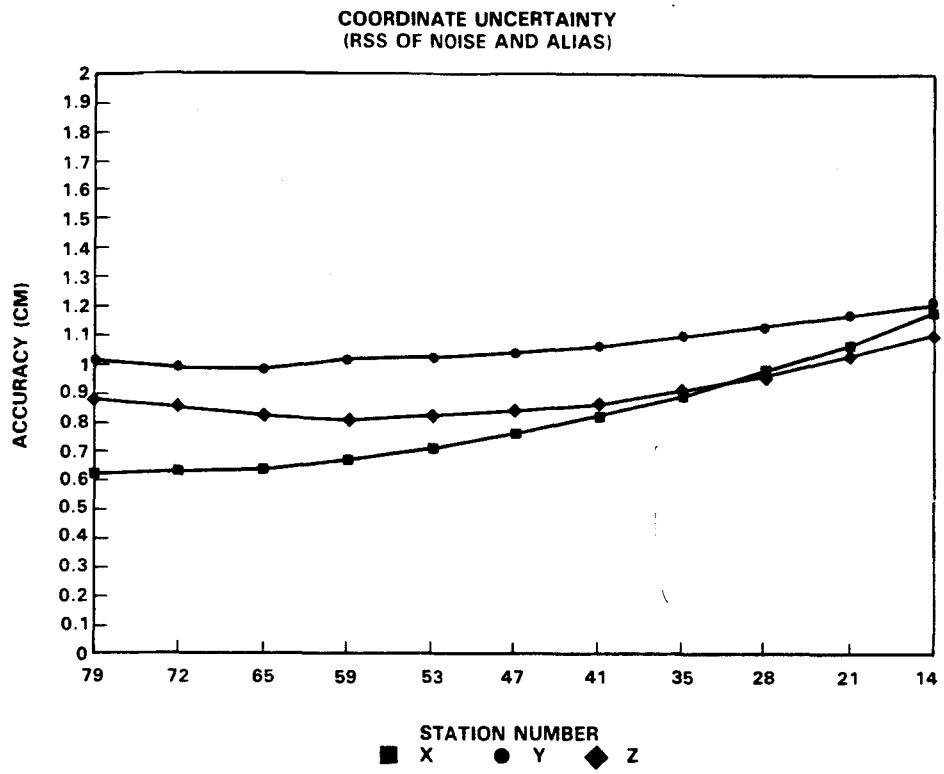

Figure 7. Uncertainties in station coordinates in an earth orbit.?

13 cm or better are expected for the Topex satellite, which will be in a much lower orbit at approximately 1300 km altitude (Stewart et al., 1986).

The preceding error analysis does not explicitly consider signal loss due to cloud cover. Partial cloud cover that only temporally obscures a target is not a major constraint. Overcast conditions are significant, however, and may put some constraints on the number of cube corners whose position is determined in a particular survey, on the minimum number of orbits required for effective data collection, or on the measurement scenario.

SUMMARY

Space-based laser geodetic measurements can be used to study a variety of fundamental geoscience phenomena. Prominent among these are crustal movements and variations in the topography of land, ice sheet, and ocean surfaces. Each of these phenomena is important to a variety of geoscience investigations ranging from understanding earthquake processes to mapping geological structures to determining the details of the hydrological cycle. In this paper we have defined a combined laser ranging and altimetry system which is capable of subcentimeter position determinations of retroflector targets and subdecimeter mapping of topography. The system uses advanced, but currently available state-of-the-art, components. Laboratory, field, and numerical experiments have indicated the suitability of the GLARS as an instrument for Eos and other space platforms.

ACKNOWLEDGEMENTS:

The GLARS study reported here is part of an ongoing analysis, system design, and mission planning effort in laser ranging and altimetry being conducted at the Goddard Space Flight Center. We acknowledge, with gratitude, the contributions to this effort of our Goddard colleagues Michael Fitzmaurice, Robert Gurney, Werner Kahn, David Smith, Maria Zuber, and H. Jay Zwally. We also thank Seth Grimes of Business and Technology Systems, Inc. for his computer programming support in the covariance analysis reported in this paper.

REFERENCES

Abshire, J. B. and C. S. Gardner, "Atmospheric refractivity corrections in satellite laser ranging," *IEEE Transactions on Geoscience and Remote Sensing*, GE-23, 414–425, 1985.

Bufton, J. L., J. E. Robinson, M. D. Femiano, and F. S. Flatow, "Satellite laser altimeter for measurement of ice-sheet topography," *IEEE Trans. on Geoscience and Remote Sensing*, GE-20(4), 544–549, 1982.

Burke, K., and T. Dixon (eds), "Final report of the Topographic Working Group," NASA, 1986.

Christodoulidis, D. C., D. E. Smith, R. Kolenkiewicz, S. M. Klosko, M. H. Torrence, and P. J. Dunn, "Observing tectonic plate motions and deformations from satellite laser ranging, *J. Geophys. Res.*, 90, 9249–9263, 1985.

Cohen, S. C., "Geophysical interpretation of satellite laser ranging measurements of crustal movement in California," *Tectonophysics*, 120, 173–189, 1985.

Cohen, S. C., and G. R. Cook "Determining crustal strain rates with spaceborne geodynamics ranging system data," *Manuscripta Geodaetica*, 4, 245–260, 1979.

Cohen, S. C., and D. E. Smith, "LAGEOS scientific results: Introduction," *J. Geophys. Res.*, 90, 9217–9220, 1985.

Cohen, S. C., and M. J. Kramer, "Crustal deformation, the earthquake cycle, and models of viscoelastic flow in the athenosphere," *Geophys. J. R. Astron. Soc.*, 78, 735–750, 1984.

Degnan, J. J., "An overview of NASA airborne and spaceborne laser ranging development," *Proceedings of the Fifth International Workshop on Laser Ranging Instrumentation*, 102–111, Royal Greenwich Observatory, East Sussex, England, 1984.

Degnan, J. J., "Satellite laser ranging: current status and future prospects," *IEEE Transactions on Geoscience and Remote Sensing*, GE-23, 398–413, 1985.

Earth Systems Sciences Committee, "Earth System Science: A Program for Global Change," NASA, Washington, 1986.

Fitzmaurice, M. W., P. O. Minott, and W. D. Kahn, "Development and testing of a spaceborne laser ranging system engineering model," NASA TM X-723-75-307, NASA, Goddard Space Flight Center, Greenbelt, MD, 1975.

Kahn, W. D., F. O. Vonbun, D. E. Smith, T. S. Englar, and B. P. Gibbs, "Performance analysis of the spaceborne laser ranging system," *Bull. Geod.*, 54, 165–180, 1980.

Kneizys, F. X., E. P. Shettle, W. O. Gallery, J. H. Chetwynd, Jr., L. W. Abreu, J. E. A. Selby, R. W. Fenn, and R. A. McClatchey, "Atmospheric transmittance/radiance: computer code LOWTRAN 6," AFGL-TR-83-0187, Air Force Geophysics Lab., Hanscom AFB, MA, 1983.

Kumar, M., and I. I. Mueller, "Detection of crustal motions using spaceborne laser ranging systems," *Bull. Geod.*, 52, 115–130, 1978.

Lambeck, K., *The Earth's Variable Rotation: Geophysical Causes and Consequences*, Cambridge University Press, London, 1980.

Lerch, F. J., S. M. Klosko, and G. B. Patel, "Gravity model development using LAGEOS," *Geophys. Res. Lett.*, 9, 1263–1266, 1982.

Leskovar, B., and B. Turko, "Optical timing receiver for the NASA spaceborne ranging system," Report LBL-8129, Lawrence Berkeley Laboratories, Berkeley, CA, 1978.

NASA, "Earth Observing System, science and mission requirements, working group report, Volume 1", NASA TM-86129, 1984.

O'Brien, H. A., "Red and near-infrared reflectance of snow," US Army Cold Regions Research and Engineering Lab Report No. 332, Hanover, NH, 1975.

Peltier, W. R., "Constraint on deep mantle viscosity from LAGEOS acceleration data," *Nature*, 304, 434–436, 1983.

Reigber, C., G. Balmino, H. Muller, W. Bosch, and B. Moynot, "GRIM gravity model improvement using LAGEOS (GRIM3-L1)", *J. Geophys. Res.*, 90, 9285–9299, 1985.

Rubincam, D. P., "Postglacial rebound observed by LAGEOS and the effective viscosity of the lower mantle," J. Geophys. Res., 89, 1077–1087, 1984.

Savage, J. C., "Strain accumulation in Western United States," *Ann. Rev. Earth Planet. Sci.*, 11, 11–43, 1983.

Seasat Special Issue II: Scientific Results, *J. Geophys. Res.*, 88, 1983.

Smith, D. E., D. C. Christodoulidis, R. Kolenkiewicz, P. J. Dunn, S. M. Klosko, M. H. Torrence, S. Fricke, and S. Blackwell, "A global reference from LAGEOS ranging (SL5.1AP," *J. Geophys. Res.*, 90, 9221–9234, 1985.

Stewart, R., L.-L. Fu, and M. Lefebvre, "Science opportunities from the Topex/Poseidon mission," NASA, Jet Propulsion Laboratory Report 86-18, Pasadena, CA, 1986.

Tapley, B. D., B. E. Schutz, and R. J. Eanes, "Station coordinates, baselines, and earth rotation from LAGEOS laser ranging: 1976–1984," *J. Geophys. Res.*, 90, 9235–9248, 1985.

Thomas, R. H., R. A. Bindschadler, R. L. Cameron, F. D. Carsey, B. Holt, T. J. Hughes, C. W. M. Swithinbank, I. M. Whillans, and H. J. Zwally, "Satellite remote sensing for ice sheet research," NASA TM 86233, 1985.

Vonbun, F. O., W. D. Kahn, P. D. Argentiero, and D. W. Koch, "Spaceborne Earth applications ranging system (SPEAR)," *J. Spacecraft and Rockets*, 14, 492–495, 1977

Wolfe, W. L., and G. J. Zissis (editors), *The Infrared Handbook*, Environmental Research Institute of Michigan, 1978.

Zagwodzki, T. W., and D. L. White, "Laboratory test results of the high speed optical tracking system for the spaceborne geodynamic ranging system" *Proceeding of the 1986 SPIE Technical Symposium Southeast on Optics and Optoelectronic Systems*, 1986.

BIBLIOGRAPHIC DATA SHEET

1. Report No. TM 87803	2. Government Accession No.	3. Recipient's Catalog No.
4. Title and Subtitle The Geoscience Laser Altimetry/Ranging System (GLARS)		5. Report Date September, 1986 6. Performing Organization Code
7. Author(s) Steven C. Cohen, John J. Degnan, Jack L. Bufton, James B. Garvin, James B. Abshire		8. Performing Organization Report No. 87B0018
9. Performing Organization Name and Address Goddard Space Flight Center Greenbelt, MD 20771		10. Work Unit No. 11. Contract or Grant No. 13. Type of Report and Period Covered
12. Sponsoring Agency Name and Address National Aeronautics and Space Administration Washington, D.C. 20540		14. Sponsoring Agency Code

15. Supplementary Notes

16. Abstract

The Geoscience Laser Altimetry/Ranging System (GLARS) is a planned highly precise laser distance measuring system to be used for geoscience measurements requiring extremely accurate geodetic observations from a space platform. The system combines the attributes of a pointable laser ranging system making observations to cube corner retroreflectors placed on the ground with those of a nadir looking laser altimeter making height observations to ground, ice sheet, and oceanic surfaces. In the ranging mode, centimeter-level precise baseline and station coordinate determinations will be made on grids consisting of 100 to 200 targets separated by distances from a few tens of kilometers to about 1000 km. These measurements will be used for studies of seismic zone crustal deformations and tectonic plate motions. Ranging measurements will also be made to a coarser, but globally distributed array of retroreflectors for both precise geodetic and orbit determination applications. In the altimetric mode, relative height determinations will be obtained with approximately decimeter vertical precision and 70–100 meter horizontal resolution. The height data will be used to study surface topography and roughness, ice sheet and lava flow thickness, and ocean dynamics. Waveform digitization will provide a measure of the vertical extent of topography within each footprint. The planned Earth Observing System is an attractive candidate platform for GLARS since the GLARS data can be used both for direct analyses and for highly precise orbit determination needed in the reduction of data from other sensors on the multi-instrument platform. Covariance error analysis for the ranging measurements indicates that subcentimeter relative point position determinations can be obtained from data acquired in 11 orbital passes (occurring in three days) over a representative cube corner network. Short arc solutions are effective in removing most of the effects of uncertainties in the gravity field, drag, and solar radiation pressure on the solution. When some of the cube corner sites are fiducial points whose positions are accurately known in a global network, then the three dimensional position of each of the target sites can be maintained to centimeter level uncertainty in the global network. Engineering analysis and experimentation indicates that a 100 picosecond, three color (1064, 532, and 355 nm) Nd:YAG laser meets the performance specifications for the system.

17. Key Words (Selected by Author(s)) laser ranging, laser altimetry, crustal movements, topography	18. Distribution Statement		
19. Security Classif. (of this report) Unclassified	20. Security Classif. (of this page) Unclassified	21. No. of Pages	22. Price*

*For sale by the National Technical Information Service, Springfield, Virginia

GSFC 25-44 (10/77)